DSS - AZOXYMETHANE (COLITIS-ASSOCIATED CANCER)

$NR3C1^{\Delta IEC}$

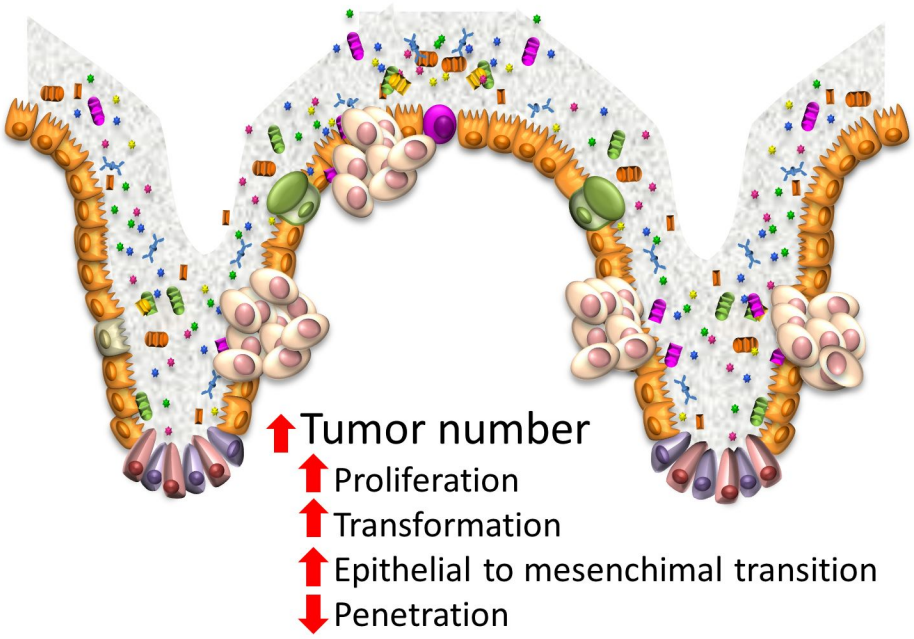

Mice carrying an epithelial deletion of the glucocorticoid receptor NR3C1 develop a higher tumor load in experimental colitis associated cancer

María Arredondo-Amador[b*], Raquel González[b*], Carlos J. Aranda[a], Olga Martínez-Augustin[a], Fermín Sánchez de Medina[b]

*Share first authorship

[a]Department of Biochemistry and Molecular Biology II, Centro de Investigación Biomédica en Red de Enfermedades Hepáticas y Digestivas (CIBERehd), School of Pharmacy, Instituto de Investigación Biosanitaria ibs.GRANADA. University of Granada, Granada, Spain

[b]Department of Pharmacology, Centro de Investigación Biomédica en Red de Enfermedades Hepáticas y Digestivas (CIBERehd), School of Pharmacy, Instituto de Investigación Biosanitaria ibs.GRANADA. University of Granada, Granada, Spain

Short title: Epithelial glucocorticoid receptor and cancer

Corresponding author: Olga Martínez Augustin, omartine@ugr.es

ABSTRACT

The glucocorticoid receptor NR3C1 is expressed in multiple cell types in the gut and elsewhere. Intestinal epithelial cells both produce and respond to glucocorticoids in different physiological and pathological contexts. In experimental colitis glucocorticoids have been shown to exert a dual role, dampening inflammation while producing a deterioration in animal status, including death. Mice with tamoxifen inducible, intestinal epithelial specific deletion of NR3C1 (NR3C1$^{\Delta IEC}$ mice) are protected against experimental colitis, suggesting glucocorticoid epithelial actions are deleterious. Since glucocorticoids modulate epithelial proliferation it follows that they may affect the development of colon cancer. In this study we set out to test this hypothesis using the dextran sulfate sodium - azoxymethane model of colitis-associated cancer. KO mice were found to exhibit a 2-fold higher tumor load but similar incidence and tumor size. Tumors had a higher trend to extend to the submucosal layer (36% vs. 0%) in NR3C1$^{\Delta IEC}$ mice, and overexpressed *Lgr5*, *Egfr* and *Myc*, consistent with increased proliferation and neoplastic transformation. *Snai1* and *Snai2* were upregulated specifically in tumors of NR3C1$^{\Delta IEC}$ mice, suggesting enhanced epithelial to mesenchymal transition in the absence of the intestinal epithelial GC receptor. We conclude that endogenous GC epithelial signaling is involved in colitis associated cancer.

KEYWORDS: glucocorticoid, azoxymethane, dextran sulfate sodium, intestinal steroidogenesis

NEW & NOTEWORTHY

- Mice carrying a tamoxifen-inducible deletion of the glucocorticoid receptor in intestinal epithelial cells ($NR3C1^{\Delta IEC}$ mice) and their corresponding controls were subjected to the azoxymethane – dextrane sulfate sodium model of colitis associated cancer
- KO mice exhibit a 2-fold higher tumor load, with a higher trend to extend to the submucosal layer (36% vs. 0%), but with similar incidence and tumor size
- Colonic tumors in $NR3C1^{\Delta IEC}$ mice showed signs of increased proliferation, neoplastic transformation and tumor associated inflammation.

INTRODUCTION

Colorectal cancer (CRC), neoplasia that affects colon or rectum, is normally originated by a progressive acquisition of genetic mutations, known as sporadic CRC. A small percentage (3-4%) appears in patients who suffer from intestinal bowel disease (IBD), a type of CRC called colitis-associated colorectal cancer (CAC). It has been amply demonstrated that chronic inflammation is a relevant risk factor for cancer, while non-steroidal anti-inflammatory drugs (NSAIDs) are able to decrease CRC incidence (5, 9). The intestinal epithelium from IBD patients is continuously submitted to active and remission stages, existing a constant alternation between inflammatory and reepithelization processes. Essentially, this causes DNA damage, promotes an hyper-proliferative state by an overstimulation of signaling pathways such as Wnt/β-catenin, allows the survival of pre-tumorigenic cells and favors the apparition of dysplasias (2). Thus, CAC arises from non-neoplasic inflammatory epithelium that progresses to cancer in the context of mutation-prone hyperproliferative epithelium. Intestinal epithelial cells (IECs) suffer what is known as epithelial-to-mesenchymal transition (EMT), a dedifferentiation process in which cells acquire mesenchymal characteristics that involve the loss of polarity and tight junctions, a cytoskeleton reorganization, and an overexpression of metalloproteases. Cells become more mobile, invasive and gain an increased ability to degrade the extracellular matrix (14). In addition to the effects of inflammation per se, IBD patients are commonly treated with immunosuppresant and immunomodulatory drugs, such as glucocorticoids (GC), which may augment CAC risk by limiting the surveillance of the immune system. Further, intestinal epithelial cells synthesize and release GC locally, and this has been claimed to collaborate in tumor immune escape (22).

Glucocorticoids (GC) are molecules with pleiotropic effects in virtually all cell types, which are attained by way of a fairly complex mechanism of action that basically depends on the interaction with its primary biological target, the cytoplasmic glucocorticoid receptor NR3C1, although nongenomic actions have also been described. Due to their potent and relatively fast anti-inflammatory and immunomodulatory actions, GC are irreplaceable in the treatment of inflammatory bouts of IBD as well as multiple other inflammatory and noninflammatory conditions. Additionally, GCs are commonly used in lymphoid cancers because of their potent anti-proliferative and apoptotic effects in this cellular type (18). In non-hematological carcinomas, they are normally only used to reduce symptoms and side-effects of chemotherapy (18). The modulatory action of NR3C1 on solid tumors remains still unclear. Even though dexamethasone revealed an ability to reverse EMT in lung epithelial cells *in vitro*, (25) there is controversy about the effects of GC in the case of CRC. Dexamethasone has nonetheless demonstrated inhibitory effects on cell growth, induction of apoptosis and enhancement of chemosensitivity in some colon cancer cell lines (13). Besides, an indirect inhibition of tumor growth by GCs was reported, due to their actions on cancer-associated fibroblasts (7). In contrast, Tian et al. assure that NR3C1 is highly activated in human metastatic colon carcinoma cell line T84. Moreover, they demonstrated that dexamethasone-dependent activation of NR3C1 promoted proliferation and invasion by inducing the Cyclin-Kinase 1. Conversely, in non-metastasic cells like HT29 line, dexamethasone effects were weaker (23).

Our group has proven that GCs impair wound healing and inhibit intestinal epithelial cell proliferation in experimental colitis, while at the same time exerting potent anti-inflammatory actions (16). Additionally, mice that carry a conditional and specific deletion of the *Nr3c1* gene in IECs ($NR3C1^{\Delta IEC}$ mice), experience an increased

epithelial proliferation, together with an inflammatory response in colon one week after deletion (1). Besides, the lack of intestinal epithelial NR3C1 protects against experimental colitis and suppresses the increased weight loss due to budesonide treatment CITA. Given the pivotal role of the epithelial NR3C1 in proliferation and inflammation, the present study will try to elucidate the involvement of intestinal epithelial NR3C1 on the development of CAC the AOM-DSS model.

MATERIALS AND METHODS.

Materials and reagents

Except where indicated, all reagents and primers were obtained from MilliporeSigma (Madrid, Spain).

Animals

C57BL/6J mice carrying lox sequences flanking the *Nr3c1* gene (B6.Cg-Nr3c1<tm1.1Jda>/J, $Nr3c1^{loxp}/Nr3c1^{loxp}$ mice) (15), supplied by Jackson Laboratories (Bar Harbor, ME, USA), were crossed with transgenic mice expressing the tamoxifen-inducible CRE recombinase under the control of the villin promoter i.e. Tg (Vill Cre/ERT2) 23Syr (Vill-Cre)(8), gently shared by Dr. Sagrario Ortega (Superior Institute of Scientific Research, Madrid, Spain) with permission of the researcher who originally generated the strain, Dr. Sylvie Robine, to obtain B6-Cg-Nr3c1-Vil-Cre/ERT2 mice, referred to in the present paper as $NR3C1^{\Delta IEC}$. To obtain the animals used in the present study, $NR3C1^{loxp/loxp}$ mice were routinely crossed with $NR3C1^{\Delta IEC}$ mice, generating offspring expressing the CRE enzyme ($NR3C1^{\Delta IEC}$) and $NR3C1^{loxp/loxp}$ mice which were used as controls and referred to as wild type. All the animals were maintained at the University of Granada Animal Facility (Biomedical Research Center, University of Granada, Granada, Spain) under SPF conditions in air-conditioned animal modules with a 12 h light-dark cycle. Mice were given free access to autoclaved tap water and standard chow (Harlan-Teklad 2014, Harlan Ibérica, Barcelona, Spain). All animal procedures in this study were carried out in accordance with the Guide for the Care and Use of Laboratory Animals as adopted and promulgated by the U.S. National Institutes of Health and were approved by the Animal Experimentation Ethics Committee of the University of Granada (ref. 01-12-14-165).

To induce the deletion of *Nr3c1* in the intestinal epithelial cells in NR3C1$^{\Delta IEC}$ mice, 1 mg tamoxifen (sunflower seed oil/ethanol mixture, 10:1 v/v) was injected intraperitoneally for 5 consecutive days (WT mice were also treated with tamoxifen).

In vivo experimental design

To induce colitis-associated colorectal cancer (CAC), the azoxymethane/dextran sodium sulfate (AOM/DSS) model was used (17). Two weeks after inducing the *Nr3c1* deletion, azoxymethane (12 mg/kg) was injected intraperitoneally to WT and NR3C1$^{\Delta IEC}$ mice (n=14-16), with a sex 1:1 ratio. After 5 days, mice were subjected to three successive 5-days cycles of DSS 2% (w/v) in drinking water, separated by 16 days intervals where DSS was replaced by water. Animals were sacrificed 75 days after AOM administration, i.e. 24 d after completion of the last DSS cycle. To ensure gene deletion throughout the experiment, tamoxifen was re-administered for 3 consecutive days 1 week after each DSS cycle.

Animal status was monitored according to the Disease Activity Index criteria (DAI) and the evolution of body weight was collected daily.

Plasmatic parameters

A blood sample was drawn intracardiacally and was spun to obtain plasma, which was snap frozen and kept at −80 °C until measurement. Plasmatic corticosterone was measured by enzyme-linked immunosorbent assay (ELISA) (Enzo Life Sciences, Farmingdale, NY) following the manufacturer's instructions.

Intestinal and extraintestinal assessment

The entire colon was removed, gently flushed with pre-cooled PBS and blotted on filter paper, placed on an ice-cold plate and cleaned of fat and mesentery. Each specimen was weighed and its length measured under a constant load (2 g). Alcian blue stain (Sigma) was added to the longitudinally opened colon to aid in tumor visualization and counting. A small segment was dissected from the distal zone of the colon and preserved in formalin for histological analysis. Subsequently, the samples destined for RNA extraction, western blot and explants were taken from both the tumor and adjacent area. The fragments were immediately frozen in liquid nitrogen and kept at −80°C until used except those destined for explant culture.

On the other hand, mesenteric lymph node cells (MLNC) were taken in order to analyze some immune cells populations by flow cytometry (see below).

Histological Assessment of Colon Damage

Distal colon tissue fragments were fixed in 4% paraformaldehyde (w/v). After being deparaffinized, sections were rehydrated in serial dilutions of ethanol and water, and stained with haematoxylin and eosin (H&E). For immunohistochemistry, deparaffinized colon tissue was incubated with 10 mM citrate buffer for 30 min at 100 ºC, washed three times in Tris Buffered Saline (Tris 50 mM and NaCl 0.15 M, TBS) for 5 min and incubated with 3% H_2O_2 in methanol for 10 min. Then, sections were washed with tap water, and IHC was performed using the Vectastain ABC kit (Vector Laboratories, Burlingame, CA, USA). The sections were blocked for 1 hour and exposed (overnight, 4 ºC) to the primary antibody to Ki67 (1:400) (Cell Signaling; Danvers, MA, USA). The tissues were then incubated with a biotinylated secondary antibody and an avidin–peroxidase complex for 30 min each, followed by incubation with Dako Real DAB+Chromogen (K5007) for staining development, for 1 minute.

For tumor index evaluation, three parameters were evaluated in a single-blind fashion: loss of epithelial structure and morphology (0-3), tumor size (0-3) and invasion degree (0= tumor circumscribed to the epithelium, 1= muscularis mucosa invasion, 2= muscularis externa invasion).

Colonic explant culture and determination of secreted cytokines by Multiplex

Two 3 mm-diameter fragments were destined for culture and immediately submerged in a PBS solution containing 500 U/mL penicillin, 0.5 mg/mL streptomycin, 12.5 µg/mL amphotericin B and 10 µg/mL gentamycin. Next, colon explants were cultured in Dulbecco's Modified Eagle's Medium (DMEM) supplemented with charcoal treated, heat-inactivated fetal bovine serum (10% v/v), 100 U/mL penicillin, 0.1 mg/mL streptomycin, 2.5 µg/mL amphotericin and 2 mM glutamine. Charcoal preexposure ensures the absence of GC in serum. After 24 h the medium was collected and snap frozen at −80 °C. TNF, VEGF, MMP9, MMP8, IL-6, MMP2, TIMP1 and MMP3 levels were measured by kit Luminex Mouse Magnetic Assay® (R&D Systems®, Minneapolis, MN).

RNA isolation and quantitative reverse-transcription polymerase chain reaction (RT-qPCR) analysis

RNA was isolated using the RNeasy minikit (Qiagen®, CA, USA) following the manufacturer's instructions. The quantity and integrity of RNA were assessed spectrophotometrically with a Nanodrop® apparatus (Thermo Scientific). Specific DNA sequences were amplified with a Biorad CFX connect real-time polymerase chain reaction (PCR) device (Alcobendas, Madrid, Spain). Primers used are shown in Table 1. Results are expressed as 2^{-ddCt} using *Ppib*, *Hprt* and *18S* as reference genes.

225

226 *Western blot analysis*

227 Tissue samples were homogenized in lysis buffer (0.1% w/v SDS, 0.1% w/v sodium
228 deoxycholate, 1% v/v Triton X-100 in PBS) with a protease inhibitor cocktail 1:200
229 (v/v) (Sigma, ref. P9599) and a phosphatase inhibitor cocktail 1:100 (v/v) (SC-45045,
230 Santa Cruz, Heidelberg, Germany). Then homogenates were sonicated and centrifuged
231 at 10,000 g/10 min/4 °C. Protein concentration was determined by the bicinchoninic
232 acid assay(4). Samples were boiled for 5 min in Laemmli buffer (Biorad), separated by
233 SDS–PAGE, electroblotted to nitrocellulose membranes (pore size 0.45 μm) (Millipore,
234 Madrid, Spain) and probed with the corresponding antibodies. The bands were detected
235 by enhanced chemiluminescence (PerkinElmer, Waltham, MA, USA). The primary
236 antibodies were generally used at a 1:1000 dilution except where indicated, and were
237 obtained from: Cell Signaling (Danvers, MA, USA) (pSTAT3 (1:2000) Ref. #9145,
238 STAT3 Ref. #9139, Cyclin D1 Ref. #2978, AKT (1:2000) Ref. #9272, pAKT (1:2000)
239 Ref. #4060, SMAD2/3 Ref. #8685, pSMAD2/3 Ref. #8828, Caspase 3 Ref. #9662, β-
240 catenin (1:4000) Ref. #9562, pβ-catenin (1:4000) Ref. #9566, MLC2 Ref. #3672):
241 Abcam (Cambrige, UK) (pMLC2 Ref. #ab2480); Developmental Studies Hybridoma
242 Bank (Iowa, USA) (Actin (1:500)). The bands were quantified with the National
243 Institute of Health software Image J.

244

245 *Flow cytometry*

246 For FACS analysis, Mesenteric lymph node cells (MLNC) cells were washed with a
247 cytometry buffer containing PBS, FBS 1 % (v/v), 0.5 mM EDTA and 0.1% sodium
248 azide (w/v). Next, cells were stained with antibodies corresponding to the following
249 markers: CD3ε-FITC, CD4-PE, FoxP3-PercP, CD8α-APC, CD19-APC, CD45-FITC,

CD11c-PercP and NK-PE. All the antibodies were from Miltenyi Biotec (Bersgisch Gladbach, Germany), eBioscience (San Diego, CA, USA) and ThermoFisher. Incubations took place for 30 min at 4ºC. Mouse Fc-Block anti-CD16/CD32 from eBioscience was added at the same time as the antibodies. For the intracellular staining of FOXP3, cells were permeabilized for 30 min with FOXP3 Staining Buffer Set (eBioscience). Stained cells were washed and fixed in PBS-paraformaldehyde 2% (w/v) 10 min at 4ºC and, after washing again, cells were resuspended in cytometry buffer for analysis with a FACSCalibur™ (BD). Cytometry data was processed with FlowJo software (Treestar, California, USA).

Data and Statistical Analysis

Results are expressed as mean ± SEM. Differences among means were tested for statistical significance by one-way ANOVA and *a posteriori* Fisher's least significant difference tests. All analyses were carried out with the GraphPad Prism 6 (La Jolla, CA, USA). Differences were considered significant at $P<0.05$.

RESULTS

The absence of NR3C1 favors a higher tumor load

CAC was induced in WT and NR3C1$^{\Delta IEC}$ mice using the AOM/DSS model. Through the 75 days of experiment, no clear differences in body weight evolution were noted between genotypes, although, initially, NR3C1$^{\Delta IEC}$ mice showed increased weight loss, also noted the very last day (Fig. 1A). A similar survival rate was observed, which was close to 80% by the end of the experimental period. DAI was similarly increased in both groups (Fig. 1D). Tumor incidence was almost 100% in both groups, with a tumor size between 1 and 4 mm (Fig. 1B). Colonic weight/length ratio was higher than normal (which is approximately 25-30 mg/cm (19)), consistent with intestinal inflammation, but was increased in WT vs. knockout mice (Fig. 1C, left). NR3C1$^{\Delta IEC}$ mice exhibited a larger number of tumors (roughly 2-fold, $P<0.05$, Fig. 1C, middle). Microscopically, the occurrence of neoplasic transformation was detected (Fig. 1E, upper row), along with vestiges of inflammation, mainly leukocyte infiltration and distortion of crypt architecture (Fig. 1E, bottom row). In most cases the tumors were confined in the mucosa, but in several instances they reached through the muscularis propia of the mucosa, all of which were observed in WT mice (Fig. 1C, right). No significant differences in epithelial structure, overall morphology or tumor size were noted (Fig. 1C, right).

In order to clarify whether intestinal epithelial NR3C1 influences the EMT process, the expression of several genes implicated in this critical step was measured by RT-qPCR in both the tumor and adjacent area samples. *Snai1* and *Snai2*, two main EMT promoting transcription factors, were upregulated in the tumor area of NR3C1$^{\Delta IEC}$ mice compared with the controls. The same trend was apparent in the adjacent tissue samples,

but without reaching significance. However, mRNA levels of epithelial and mesenchymal markers did not correlate with *Snai1* and *2* expression. Thus *Cdh1* and *Tjp1*, which encode the epithelial specific proteins E-cadherin and ZO-1, respectively, were increased in the absence of NR3C1 (Fig. 2A), while *Vim* (vimentin), a marker of mesenchymal cells, was upregulated in the adjacent area samples obtained from WT mice compared to NR3C1$^{\Delta IEC}$, with no differences in tumoral tissue. Following the same profile as E-cadherin and ZO-1, a rise in *Tgfb1* and *Smad7* expression was detected in the tumors of knockout mice (Fig. 2), suggesting a pronounced activation of EMT triggered by the absence of the NR3C1 receptor (24). *Tgfb1* was upregulated even in the tumor adjacent area. Nevertheless, the phosphorylation of SMAD2/3, which is downstream in of TGF-β receptor activation, was unaffected by NR3C1 status (Fig. 2B).

NR3C1$^{\Delta IEC}$ colons present an altered proliferative status

Genes related to cellular cycle and proliferation were evaluated in the colon from WT and NR3C1$^{\Delta IEC}$ to assess the possible correlation with the higher tumor load associated to the deletion of NR3C1. *Lgr5* (leucine-rich repeat-containing G-protein coupled receptor 5), a marker of intestinal stem cells; *Egfr* (epidermal growth factor receptor); and *cMyc* (MYC), all followed the same profile, i.e. increased expression in tumor samples of NR3C1$^{\Delta IEC}$ mice compared with tumor samples from WT mice, as well as with their adjacent area (Fig. 3A). According to these results, a hyper-proliferative status is evidenced in NR3C1$^{\Delta IEC}$ mice. Curiously, the absence of NR3C1 did not result in changes in cyclin D1 protein levels, which are normally upregulated by MYC and LGR5, nor in β-catenin phosphorylation, one of the main pathways altered in CAC (Fig. 3B). Similarly, the expression of *Nr5a2* (encoding LRH1), involved not only in epitelial

proliferation but also in steroidogenesis, was downregulated in the tumors of WT mice to a level comparable to that of KO mice (Fig. 5D). Lastly, immunohistochemistry of Ki67 was conducted in colon samples. No differences were noted between genotypes (Fig. 3C).

Increased inflammation in tumors from NR3C1$^{\Delta IEC}$ mice

To evaluate the inflammatory status of mice, *Hp* (haptoglobin), *S100a9* (S100A9), *Ptgs2* (COX2) and *Nos2* (iNOS) were measured in colon by RT-qPCR. It was found that *Hp*, *S100a9* and *Ptgs2* were overexpressed by tumors in both WT and knockout mice, with *Nos2* showing a similar albeit nonsignificant trend (Fig. 4A). Moreover, *Hp*, *S100a9* and *Nos2* were significantly upregulated in tumors from NR3C1$^{\Delta IEC}$ compared to WT mice. Consistent with this notion, *Ifng* (encoding IFN-γ) mRNA levels were also higher in knockout tumor tissue (just short of significance, p=0.06, Fig. 4B). *Il10* was unchanged in tumor samples, but was upregulated in the adjacent tissue of NR3C1$^{\Delta IEC}$ mice (Fig. 4B). Taken together, these data indicate that the colonic tumors are associated with an inflammatory state, and more so in the context of reduced expression of the GC receptor. The colonic phosphorylation of STAT3 was also evaluated, as it can be induced by IL6. In this case, no differences were observed (Fig. 4C).

Given that the immune system plays a pivotal role in the development of cancer, mesenteric leukocyte populations were evaluated by flow cytometry. No differences were observed in the macrophages, B lymphocytes (data not shown), CD4+, CD8+ or Treg lymphocytes (Fig. 5A). The only change observed at this level was an increased percentage of NK cells in NR3C1$^{\Delta IEC}$ mice (Fig. 5B). Thus this aspect was not investigated further.

Intestinal steroidogenesis is unchanged in the absence of epithelial glucocorticoid receptor

It has been shown that, unlike normal intestinal epithelial cells, colonic cancer cells constitutively synthetize GC in basal conditions, and this endogenous GC output may play an important role in the evasion from the immune system by tumor cells i.e. immune escape (21). In order to assess steroidogenesis in our model, plasmatic levels as well as the synthesis of corticosterone by colonic explants in vitro were assessed in WT and NR3C1$^{\Delta IEC}$ mice. As shown in Fig. 5C, plasma corticosterone levels were comparable in both genotypes. More importantly, colonic synthesis of the steroid was similar in explants obtained from the tumor or the tumor adjacent tissue, and there was no effect of NR3C1 status or *Nr5a2* expression (Fig. 5D).

Other changes related to angiogenesis and extracellular matrix dynamics

As tumor growth depends on angiogenesis, which can be promoted by extracellular matrix degradation, *Vegfa* (vascular endothelial growth factor A, VEGF) and *Mmp9* expression was assessed by RT-qPCR. In both cases, the lack of NR3C1 gave rise to an increased expression in the tumor area compared to WT mice. In addition, the levels of *Mmp9* expression were higher in tumor vs. adjacent area (Fig. 6A). It should be noted however that VEGF and MMP9 protein levels were not significantly different in explant supernatants, although a trend to increase in knockout specimens was observed in the latter case (Fig. 6B, upper, middle). These changes may be related to the fact that explants were obtained from an area farther removed from the tumor than the RNA sample. Lastly, there were no differences in MMP2 or 8 nor in TIMP1, an inhibitor of metalloproteases, although a decrease in MMP3 levels was observed in NR3C1$^{\Delta IEC}$ mice (Fig. 6B).

DISCUSSION

In this report, we demonstrate that the intestinal epithelial GC receptor NR3C1 plays a significant role in colitis associated colorectal cancer in the AOM/DSS murine model, with a major impact on the number of tumors, which was duplicated in $NR3C1^{\Delta IEC}$ mice. Euthanasia of animals occurred 24 days after the last cycle of DSS, a moment in which a high incidence of tumors and a low level of inflammation in the colon was expected. The former is the consequence of a relatively long follow up period after the initial genotoxic insult (AOM) using a dose long established to induce colonic tumors with high penetrance (virtually 100% in the present study). The repeated cycles of DSS exposure reproducibly result in chronic colitis, but typically the severity of inflammation is lower than that in the acute version (i.e. 7 days of DSS), and is partially dampened after a sufficiently long DSS-free period, as in this case. While the present study was focused on CAC rather than colitis itself, the inflammatory reaction is highlighted by weight loss in the first DSS cycle, increased DAI, by the histological findings, and by the colonic weight/length ratio, which was increased over reference normal values. In addition, body weight remained relatively stable after the initial loss over the remaining 70 d period, instead of the progressive gain that would be expected in healthy mice, consistent with low grade, chronic colitis.

We have previously shown that intestinal epithelial NR3C1 deletion is protective in experimental colitis, except in the very early stages of DSS administration (unpublished observations). Consistent with protection against colitis, colonic weight to length ratio was significantly reduced in knockout mice at the end of the experimental period, although it was still higher than normal values (approximately 25-30 mg/cm). Given the established association between chronic inflammation and colonic carcinogenesis, the attenuated inflammatory status of $NR3C1^{\Delta IEC}$ mice would be expected to result in a

diminished tumor yield. In fact, the opposite result was obtained i.e. knockout mice presented a higher (2-fold) tumor load, highlighting the importance of this signaling pathway in tumorigenesis. There were no differences in CAC incidence, which as noted was virtually 100%, and average tumor size was similar in both groups. Histologically, tumors exhibited comparable characteristics in WT and NR3C1$^{\Delta IEC}$ mice, except for their tendency to extend to the base of the mucosa. Thus in 36% of WT samples the tumor reached through the muscularis mucosa to the submucosa, a sign of invasivity. Notably, this feature was totally absent in NR3C1$^{\Delta IEC}$ mice.

Our data further indicate that tumors from the NR3C1$^{\Delta IEC}$ group overexpress *Lgr5*, *Egfr* and *Myc.* Increased levels of *Lgr5* (encoding the LGR5 cell marker) suggest expansion of stem cells, while EGFR (encoded by *Egfr*) is the epithelial growth factor receptor, overexpressed in several types of cancer. Moreover, monoclonal antibodies against EGFR such as cetuximab and pananitumumab are used in the treatment of RAS-wild type metastatic CRC (10). c-*Myc* is an oncogene implicated in cell cycle and survival which is often aberrantly expressed in CRC. These changes are consistent with enhanced carcinogenesis and are specifically linked to the tumors present in NR3C1$^{\Delta IEC}$ mice, i.e. they were not detected in tumors obtained from WT mice (taking the adjacent tissue as reference). They are also suggestive of increased epithelial proliferation, which would be expected given the known epithelial anti-proliferative effects of GCs and our previous results on the deletion of the receptor in basal conditions (1). However, it should be noted that no differences were found in the protein levels of cyclin D1 between WT and knockout mice. Further, Ki67 staining was comparable in both groups. Consistent with these changes, the increased expression of *Snai1* and *Snai2* in the tumors of NR3C1$^{\Delta IEC}$ mice points to enhanced epithelial to mesenchymal transition in the absence of the intestinal epithelial GC receptor. Again, this is an effect observed

415 solely in knockout mice i.e. there was strictly no change in the controls. Interestingly,
416 the epithelial markers *Cdh1* and *Tjp1*, encoding E-cadherin and ZO-1, were found to be
417 overexpressed in knockout animals. However, this feature was present in both the tumor
418 and the adjacent area, suggesting that it is related to gene deletion more than to tumor
419 formation. Whether or to which extent this may oppose EMT is unknown. The
420 expression of vimentin, a marker of mesenchymal cells, was found to be differentially
421 regulated in WT and knockout mice, as it was downregulated in WT tumors but
422 upregulated in NR3C1$^{\Delta IEC}$ tumors. Since vimentin is increased in the adjacent area
423 samples of WT mice, mRNA levels turned out to be comparable in tumors of both
424 groups. Augmented tumor peripheral vimentin may thus be involved in enhanced
425 invasivity, as it is able to participate in the evasion from degradation of proteins like
426 SCRIB, which promotes direct cell migration and invasion (20).
427 TGFβ is a cytokine with opposite effects in tumorigenesis depending on the phase of the
428 illness. In the early stages, TGFβ inhibits the proliferation of intestinal cells and
429 maintains their differentiated state, while at later stages, when cells already exhibit
430 malignant features like accumulation of mutations and increased survival and
431 proliferation, TGFβ favors EMT by promoting SNAIL1 and SNAIL2 overexpression
432 (12). Suppression of epithelial NR3C1 expression results in an increase in the mRNA
433 levels of this cytokine. However, phosphorylation of SMAD2/3, which is downstream
434 of TGFβ receptor signaling, as assessed by Western blot, was unaffected. Further, the
435 expression of SMAD7, an inhibitor of this signaling pathway, was augmented at the
436 mRNA level in tumor samples of knockout mice. In addition, *Tgfb* was similarly
437 increased in tumor and surrounding tissue of NR3C1$^{\Delta IEC}$ mice compared with the
438 controls. Thus the role of TGFβ in the promotion of EMT in knockout animals is
439 uncertain at this point.

Analysis of inflammatory markers in the tumor vs. adjacent samples reveals that tumor formation is associated with a local inflammatory response, as indicated by increased haptoglobin (*Hp*), S100A9 (*S100a9*) or COX2 (*Ptgs2*). This profile was observed in both WT and NR3C1$^{\Delta IEC}$ mice, but the inflammatory response was more pronounced in the latter group, based on increased expression of *Hp*, *S100a9* and *Nos2*. *Ptgs2* and *Ifng* mRNA levels were also higher in tumors of knockout vs. WT mice, but without reaching significance (P=0.06 for the latter). This augmented inflammatory response is strictly confined to the tumor, and therefore not inconsistent with dampened colitis status in the absence of NR3C1 as stated above. We found no major changes in the leukocyte main types in mesenteric lymph nodes. This population was assessed as a proxy to mucosal cells, which could not be directly evaluated.

Extracellular matrix degradation and remodeling is essential for cancer cell proliferation and migration. Matrix metalloproteinases (MMPs) play a crucial role in this process, as they are proteolytic enzymes able to degrade it. Commonly they are correlated with CRC invasion, but anti-tumorigenic effects had been recently attributed also to MMPs (6). MMP3 is downregulated in the absence of epithelial NR3C1. Although the functional role of MMP3 in colorectal cancer needs to be elucidated, it seems that MMP3 contributes to the invasive character of tumors (3), which would be consistent with the reduced invasion from NR3C1$^{\Delta IEC}$ tumors. On the other hand, tumors from NR3C1$^{\Delta IEC}$ mice overexpress *Mmp9*. This metalloproteinase participates in pro-inflammatory responses during colitis, while both anti-tumor and pro-tumorigenic actions have been attributed in CAC, although MMP9$^{-/-}$ mice are more susceptible to CAC (11). Thus the role of MMP9 in increased tumorigenesis in NR3C1$^{\Delta IEC}$ mice is uncertain.

Culture supernatants from colonic explants maintained in GC free medium contained significant amounts of corticosterone, consistent with the known steroidogenic capacity of intestinal epithelial cells. Colonic tumors have been reported to exhibit an increased GC output, which could be involved in immune escape. In this case, however, corticosterone levels were comparable in tumor and adjacent tissue explants. Although this is not supportive of increased GC production by the tumor, our use of surrounding tissue as reference constitutes a limitation, inasmuch as steroidogenesis may extend beyond the tumor edge. Corticosterone levels were also similar in WT and $NR3C1^{\Delta IEC}$ mice. In a previous study we found that local steroidogenesis is increased in $NR3C1^{\Delta IEC}$ mice after induction of DSS colitis, suggesting the GC receptor is involved in a negative feedback regulatory loop (unpublished observations). Thus our data indicate that steroidogenesis is not regulated by the receptor in our experimental setting, perhaps because inflammation is less intense than in the standard 7 day DSS protocol.

Taken together, our data indicate that the absence of the intestinal epithelial GC receptor, NR3C1, doubles the number of tumors in the AOM-DSS CAC model and increases the expression of tumoral, EMT and inflammatory markers, despite of a lower degree of colonic inflammation. The underlying cause appears to be related to tumor promotion rather than immune escape, possibly related to increased early proliferation. The tumors appear to be less invasive in knockout animals.

GRANTS

This work was supported by funds from the Ministry of Economy and Competitivity, partly with Fondo Europeo de Desarrollo Regional (FEDER) funds [SAF2017-88457-R, AGL2017-85270-R, BFU2014-57736-P, AGL2014-58883-R] and by Junta de Andalucía [CTS235, CTS164]. MA and CJA were supported by the University of Granada (Contrato Puente Program - Plan Propio) and the Ministry of Education [Spain], respectively. CIBERehd is funded by Instituto de Salud Carlos III.

DISCLOSURES

No conflicts of interest, financial or otherwise, are declared by the authors.

AUTHOR CONTRIBUTIONS

MAA, RG and CJA performed experiments; MAA and RG analyzed data, prepared figures and drafted the manuscript; OMA and FSM conceived and designed research; all authors interpreted the results, edited, revised and approved the final version of the manuscript.

504

505 **Table 1.** Primers used in the RT-qPCR analysis.

Gen	**Forward 5'-3'**	**Reverse 3'-5'**
18s	TGGTGGAGCGATTTGTCTGG	ACGCTGAGCCAGTCAGTGTACG
Birc5	TAGAGGAGCATAGAAAGCAC	CTCTTTTTGCTTGTTGTTGG
Cdh1	CATGTTCACTGTCAATAGGG	GTGTATGTAGGGTAACTCTCTC
Egfr1	CTGTCGCAAAGTTTGTAATG	GAATTTCTAGTTCTCGTGGG
Hp	ATGGACTTTGAAGATGACAG	GTAGTCTGTAGAACTGTCGG
Hprt	AGGGATTTGAATCACGTTTG	TTTACTGGCAACATCAACAG
Ifng	TGAGTATTGCCAAGTTTGAG	CTTATTGGGACAATCTCTTCC
Il10	CAGGACTTTAAGGGTTACTTG	ATTTTCACAGGGGAGAAATC
Lgr5	AGAACACTGACTTTGAATGG	CACTTGGAGATTAGGTAACTG
Mmp9	CTTCCAGTACCAAGACAAAG	ACCTTGTTCACCTCATTTTG
Myc	TTTTGTCTATTTGGGGACAG	CATAGTTCCTGTTGGTGAAG
Nr5a2	TTGAGTGGGCCAGGAGTAGT	ACGCGACTTCTGTGTGTGAG
Ppib	CAAATCCTTTCTCTCCTGTAG	TGGAGATGAATCTGTAGGAC
S100a9	CTTTAGCCTTGAGCAAGAAG	TCCTTCCTAGAGTATTGATGG
Smad7	CTCTGTGAACTAGAGTCTCC	GAAGTTGGGAATCTGAAAGC
Snai1	AGTTGACTACCGACCTTG	AAGGTGAACTCCACACAC
Snai2	GACACATTAGAACTCACACTG	GACATTCTGGAGAAGGTTTTG
Tjp1	GGGGCCTACACTGATCAAGA	TGGAGATGAGGCTTCTGCTT
Tnf	CGTGGAACTGGCAGAAGAGG	CAGGAATGAGAAGAGGCTGAGAC
Vegfa	TAGAGTACATCTTCAAGCCG	TCTTTCTTTGGTCTGCATTC
Vim	GAACCTGAGAGAAACTAACC	GATGCTGAGAAGTCTCATTG

506

507 REFERENCES

508

509 1. **Aranda CJ, Arredondo-Amador M, Ocon B, Lavin JL, Aransay AM,**
510 **Martinez-Augustin O, and Sanchez de Medina F.** Intestinal epithelial deletion of the
511 glucocorticoid receptor NR3C1 alters expression of inflammatory mediators and barrier
512 function. *Faseb j* 33: 14067-14082, 2019.
513 2. **Beaugerie L and Itzkowitz SH.** Cancers Complicating Inflammatory Bowel
514 Disease. *N Engl J Med* 373: 195, 2015.
515 3. **Bufu T, Di X, Yilin Z, Gege L, Xi C, and Ling W.** Celastrol inhibits colorectal
516 cancer cell proliferation and migration through suppression of MMP3 and MMP7 by the
517 PI3K/AKT signaling pathway. *Anti-cancer drugs* 29: 530-538, 2018.
518 4. **Canny G, Swidsinski A, and McCormick BA.** Interactions of intestinal
519 epithelial cells with bacteria and immune cells: methods to characterize microflora and
520 functional consequences. *Methods Mol Biol* 341: 17-35, 2006.
521 5. **Chan AT, Ogino S, and Fuchs CS.** Aspirin and the risk of colorectal cancer in
522 relation to the expression of COX-2. *N Engl J Med* 356: 2131-2142, 2007.
523 6. **Decock J, Thirkettle S, Wagstaff L, and Edwards DR.** Matrix
524 metalloproteinases: protective roles in cancer. *Journal of cellular and molecular*
525 *medicine* 15: 1254-1265, 2011.
526 7. **Drebert Z, De Vlieghere E, Bridelance J, De Wever O, De Bosscher K,**
527 **Bracke M, and Beck IM.** Glucocorticoids indirectly decrease colon cancer cell
528 proliferation and invasion via effects on cancer-associated fibroblasts. *Experimental cell*
529 *research* 362: 332-342, 2018.

8. **el Marjou F, Janssen K-P, Chang BH-J, Li M, Hindie V, Chan L, Louvard D, Chambon P, Metzger D, and Robine S.** Tissue-specific and inducible Cre-mediated recombination in the gut epithelium. *Genesis* 39: 186-193, 2004.

9. **Flossmann E, Rothwell PM, British Doctors Aspirin T, and the UKTIAAT.** Effect of aspirin on long-term risk of colorectal cancer: consistent evidence from randomised and observational studies. *Lancet* 369: 1603-1613, 2007.

10. **Fornasier G, Francescon S, and Baldo P.** An Update of Efficacy and Safety of Cetuximab in Metastatic Colorectal Cancer: A Narrative Review. *Advances in therapy* 35: 1497-1509, 2018.

11. **Garg P, Sarma D, Jeppsson S, Patel NR, Gewirtz AT, Merlin D, and Sitaraman SV.** Matrix metalloproteinase-9 functions as a tumor suppressor in colitis-associated cancer. *Cancer Res* 70: 792-801, 2010.

12. **Hao Y, Baker D, and Ten Dijke P.** TGF-beta-Mediated Epithelial-Mesenchymal Transition and Cancer Metastasis. *Int J Mol Sci* 20, 2019.

13. **He J, Zhou J, Yang W, Zhou Q, Liang X, Pang X, Li J, Pan F, and Liang H.** Dexamethasone affects cell growth/apoptosis/chemosensitivity of colon cancer via glucocorticoid receptor alpha/NF-kappaB. *Oncotarget* 8: 67670-67683, 2017.

14. **Lamouille S, Xu J, and Derynck R.** Molecular mechanisms of epithelial-mesenchymal transition. *Nature reviews Molecular cell biology* 15: 178-196, 2014.

15. **Mittelstadt PR, Monteiro JP, and Ashwell JD.** Thymocyte responsiveness to endogenous glucocorticoids is required for immunological fitness. *J Clin Invest* 122: 2384-2394, 2012.

16. **Ocon B, Aranda CJ, Gamez-Belmonte R, Suarez MD, Zarzuelo A, Martinez-Augustin O, and Sanchez de Medina F.** The glucocorticoid budesonide has

554 protective and deleterious effects in experimental colitis in mice. *Biochem Pharmacol*
555 116: 73-88, 2016.
556 17. **Parang B, Barrett CW, and Williams CS.** AOM/DSS Model of Colitis-
557 Associated Cancer. *Methods Mol Biol* 1422: 297-307, 2016.
558 18. **Pufall MA.** Glucocorticoids and Cancer. *Adv Exp Med Biol* 872: 315-333, 2015.
559 19. **Sanchez de Medina F, Martinez-Augustin O, Gonzalez R, Ballester I, Nieto**
560 **A, Galvez J, and Zarzuelo A.** Induction of alkaline phosphatase in the inflamed
561 intestine: a novel pharmacological target for inflammatory bowel disease. *Biochem*
562 *Pharmacol* 68: 2317-2326, 2004.
563 20. **Satelli A and Li S.** Vimentin in cancer and its potential as a molecular target for
564 cancer therapy. *Cell Mol Life Sci* 68: 3033-3046, 2011.
565 21. **Sidler D, Renzulli P, Schnoz C, Berger B, Schneider-Jakob S, Fluck C,**
566 **Inderbitzin D, Corazza N, Candinas D, and Brunner T.** Colon cancer cells produce
567 immunoregulatory glucocorticoids. *Oncogene* 30: 2411-2419, 2011.
568 22. **Sidler D, Renzulli P, Schnoz C, Berger B, Schneider-Jakob S, Flück C,**
569 **Inderbitzin D, Corazza N, Candinas D, and Brunner T.** Colon cancer cells produce
570 immunoregulatory glucocorticoids. *OncoImmunology* 1: 529-530, 2012.
571 23. **Tian D, Tian M, Han G, and Li J-L.** Increased glucocorticoid receptor activity
572 and proliferation in metastatic colon cancer. *Scientific Reports* 9: 11257, 2019.
573 24. **Troncone E, Marafini I, Stolfi C, and Monteleone G.** Transforming Growth
574 Factor-β1/Smad7 in Intestinal Immunity, Inflammation, and Cancer. *Frontiers in*
575 *immunology* 9: 1407-1407, 2018.
576 25. **Zhang L, Lei W, Wang X, Tang Y, and Song J.** Glucocorticoid induces
577 mesenchymal-to-epithelial transition and inhibits TGF-beta1-induced epithelial-to-
578 mesenchymal transition and cell migration. *FEBS letters* 584: 4646-4654, 2010.

579 **FIGURE LEGENDS**

580

581 **Figure 1.** Colonic status after azoxymethane/dextran sodium sulfate (AOM/DSS)
582 exposure of WT and NR3C1$^{\Delta IEC}$ mice. A. Body weight evolution, expressed as
583 percentage of initial weight. B. Representative images of the macroscopic appearance of
584 colons (tumors marked with arrowheads). C. Colonic weight/length ratio (left); number
585 of tumors (middle); tumoral index of histological sections of colons (right). Parameters
586 were evaluated in a single-blind fashion. D. Disease Activity Index (DAI) (left),
587 survival curve (right). E. Representative histological sections of colons (hematoxylin &
588 eosin staining). Experimental group size: n=9-11. AU= Arbitrary Units. $^{+}P < 0.05$ *vs*.
589 WT.

590

591 **Figure 2.** Expression of genes related to Epithelial-to-Mesenchymal Transition of colon
592 tissue from WT and NR3C1$^{\Delta IEC}$ mice exposed to AOM/DSS. A. Relative expression of
593 *Snai1*, *Snai2* and *Tjp1* (upper); *Cdh1* (middle), *Vim* and *Tgfb1* (bottom) assessed by RT-
594 qPCR (n=9-11). *Ppib* and *18S* were used as reference genes. B. Relative expression of
595 *Smad7* (left) assessed by RT-qPCR (n=9-11). *Ppib* and *18S* were used as reference
596 genes. SMAD2/3 phosphorylation assessed by Western blot (n=6). Samples were
597 colonic tumoral tissue (Tumor) and tissue adjacent to the tumor (Adjacent). AU=
598 Arbitrary Units. $^{+}P<0.05$ NR3C1$^{\Delta IEC}$ *vs*. WT; $*P<0.05$ Tumor *vs*. Adjacent.

599

600 **Figure 3.** Epithelial proliferation in the colon of WT and NR3C1$^{\Delta IEC}$ mice exposed to
601 AOM/DSS. A. Relative expression of *Lgr5* (left), *Egfr* (middle) and *cMyc* (right)
602 assessed by RT-qPCR (n=9-11). *Ppib* and *18S* were used as reference genes. B. Colonic
603 cyclin D1 expression and β-catenin phosphorylation assessed by Western blot (n=6).

Samples were colonic tumoral tissue (Tumor) and tissue adjacent to the tumor (Adjacent). C. Representative images of Ki67 immunohistochemistry of colon sections. AU= Arbitrary Units. $^{+}P<0.05$ NR3C1$^{\Delta IEC}$ *vs*. WT; *$P<0.05$ Tumor *vs*. Adjacent.

Figure 4. Inflammatory status of the colon from WT and NR3C1$^{\Delta IEC}$ mice exposed to AOM/DSS. A. Relative expression of *Hp*, *S100a9*, *Ptgs2* and *Nos2* assessed by RT-qPCR (n=9-11). *Ppib* and *18S* were used as reference genes. Samples were colonic tumoral tissue (Tumor) and tissue adjacent to the tumor (Adjacent). B. STAT3 phosphorylation assessed by Western blot (n=6). C. Relative expression of *Il10* and *Ifng* assessed by RT-qPCR (n=9-11). *Ppib* and *18S* were used as reference genes. AU= Arbitrary Units. $^{+}P<0.05$ NR3C1$^{\Delta IEC}$ *vs*. WT; *$P<0.05$ Tumor *vs*. Adjacent.

Figure 5. Relative leukocyte mesenteric populations and plasmatic and intestinal corticosterone levels of WT and NR3C1$^{\Delta IEC}$ mice exposed to AOM/DSS. Mesenteric leukocyte populations were measured by flow cytometry. A. CD4+T lymphocytes (gate CD3+) (upper, left); Treg lymphocytes (FoxP3+) (gate CD3+CD4+) (Upper, right); CD8+T lymphocytes (gate CD3+) (bottom, left) (n=9-11). B. NK cells (NK+) (gate CD45+) (n=9-11). C. Plasmatic corticosterone (left) and corticosterone release by colonic explants (right) measured by ELISA (n=11-12). D. Relative expression of *Nr5a2* assessed by RT-qPCR (n=9-11). *Ppib* and *18S* were used as reference genes. Samples were colonic tumoral tissue (Tumor) and tissue adjacent to the tumor (Adjacent). $^{+}P<0.05$ NR3C1$^{\Delta IEC}$ *vs*. WT; *$P<0.05$ Tumor *vs*. Adjacent.

Figure 6. Parameters related to angiogenesis and extracellular matrix dynamics. A. Relative expression of *Vegf* (left) and *Mmp9* (left) assessed by RT-qPCR (n=9-11). *Ppib*

629 and *18S* were used as reference genes. Samples were colonic tumoral tissue (Tumor)
630 and tissue adjacent to the tumor (Adjacent). B. Cytokine release by colonic explants by
631 multiplex analysis. $^{+}P<0.05$ $NR3C1^{\Delta IEC}$ *vs*. WT; $*P<0.05$ Tumor *vs*. Adjacent.
632
633
634

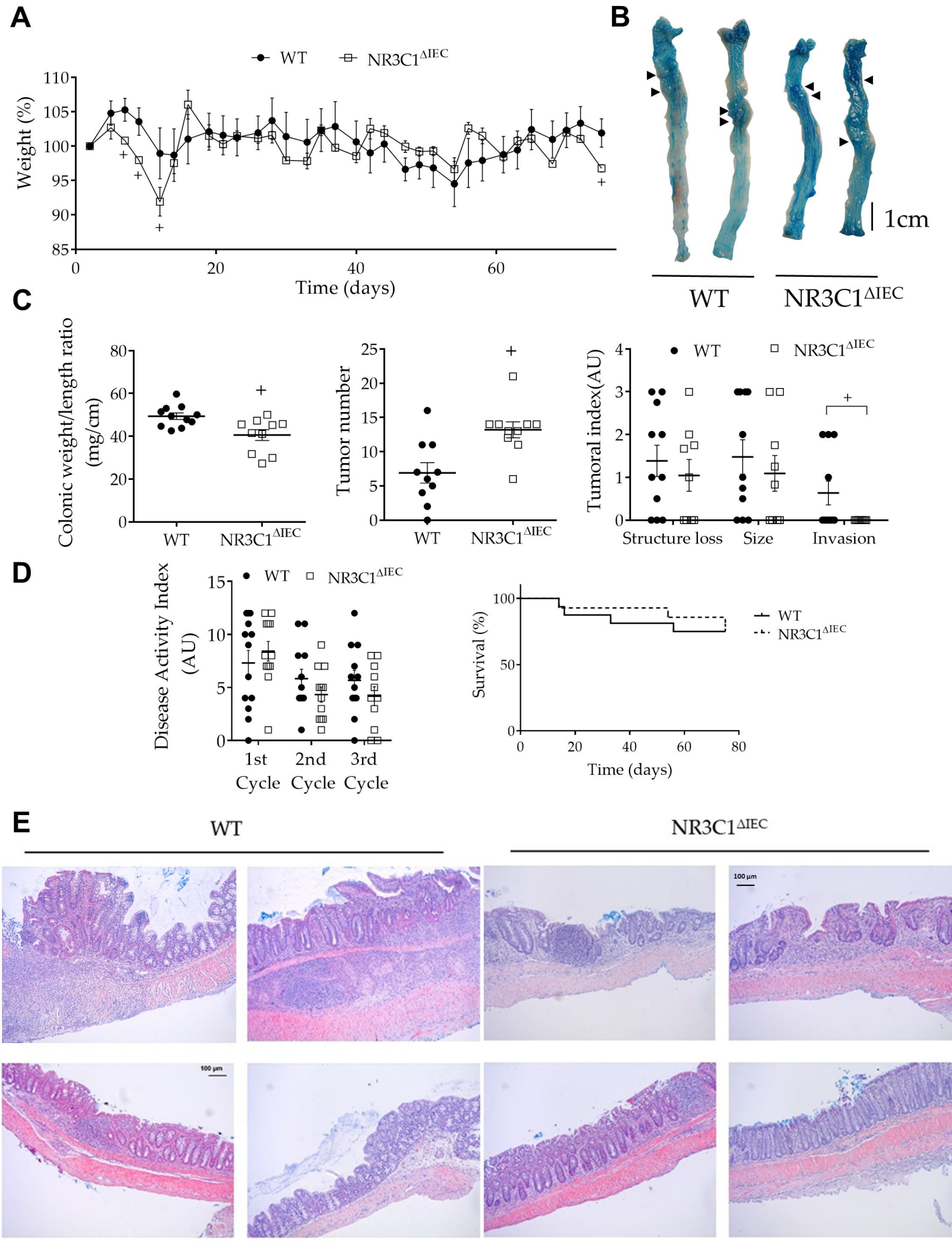
A
WT
NR3C1ΔIEC
Weight (%)
Time (days)
B
1cm
WT
NR3C1ΔIEC
C
Colonic weight/length ratio (mg/cm)
Tumor number
Tumoral index(AU)
Structure loss
Size
Invasion
D
Disease Activity Index (AU)
1st Cycle
2nd Cycle
3rd Cycle
Survival (%)
Time (days)
E
WT
NR3C1ΔIEC
100 µm

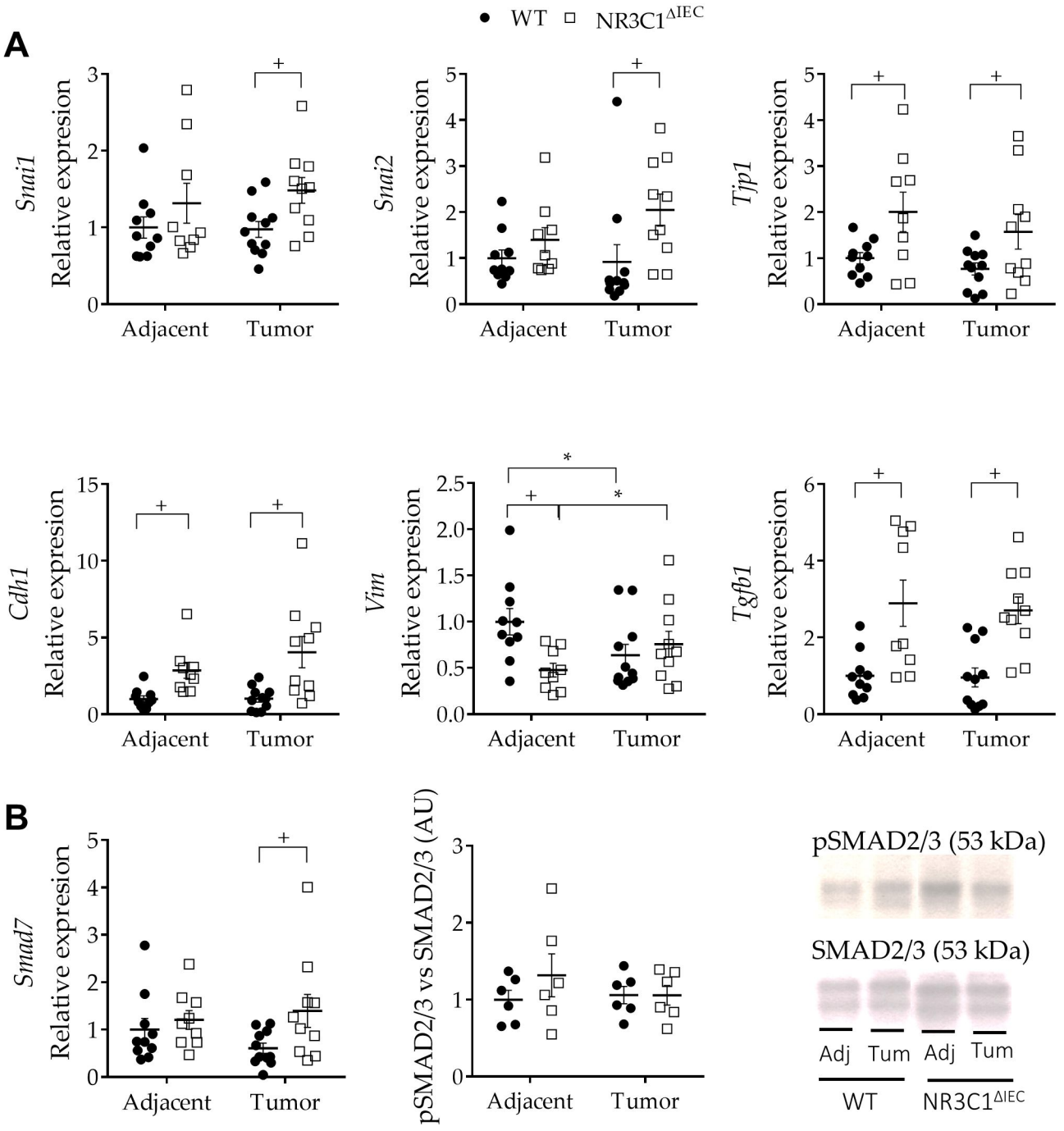
WT
NR3C1ΔIEC
A
Snai1
Relative expresion
Snai2
Relative expresion
Tjp1
Relative expresion
Cdh1
Relative expresion
Vim
Relative expresion
Tgfb1
Relative expresion
Adjacent
Tumor
B
Smad7
Relative expresion
pSMAD2/3 vs SMAD2/3 (AU)
pSMAD2/3 (53 kDa)
SMAD2/3 (53 kDa)
Adj
Tum
Adj
Tum
WT
NR3C1ΔIEC

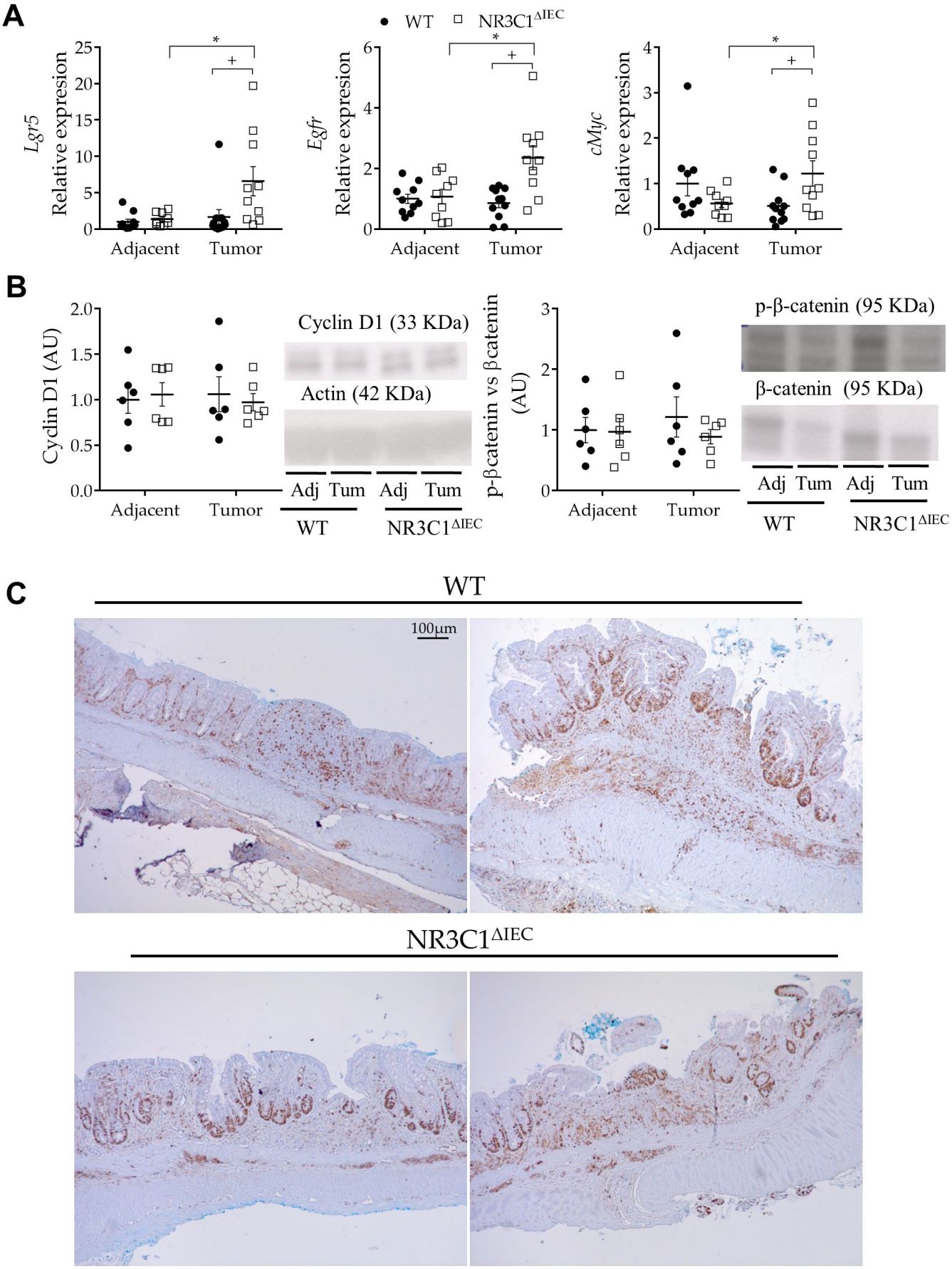
A
WT
NR3C1ΔIEC
Lgr5
Relative expresion
Egfr
Relative expresion
cMyc
Relative expresion
Adjacent
Tumor
B
Cyclin D1 (AU)
Cyclin D1 (33 KDa)
Actin (42 KDa)
Adj Tum Adj Tum
WT
NR3C1ΔIEC
p-β-catenin vs βcatenin (AU)
p-β-catenin (95 KDa)
β-catenin (95 KDa)
C
WT
100μm
NR3C1ΔIEC

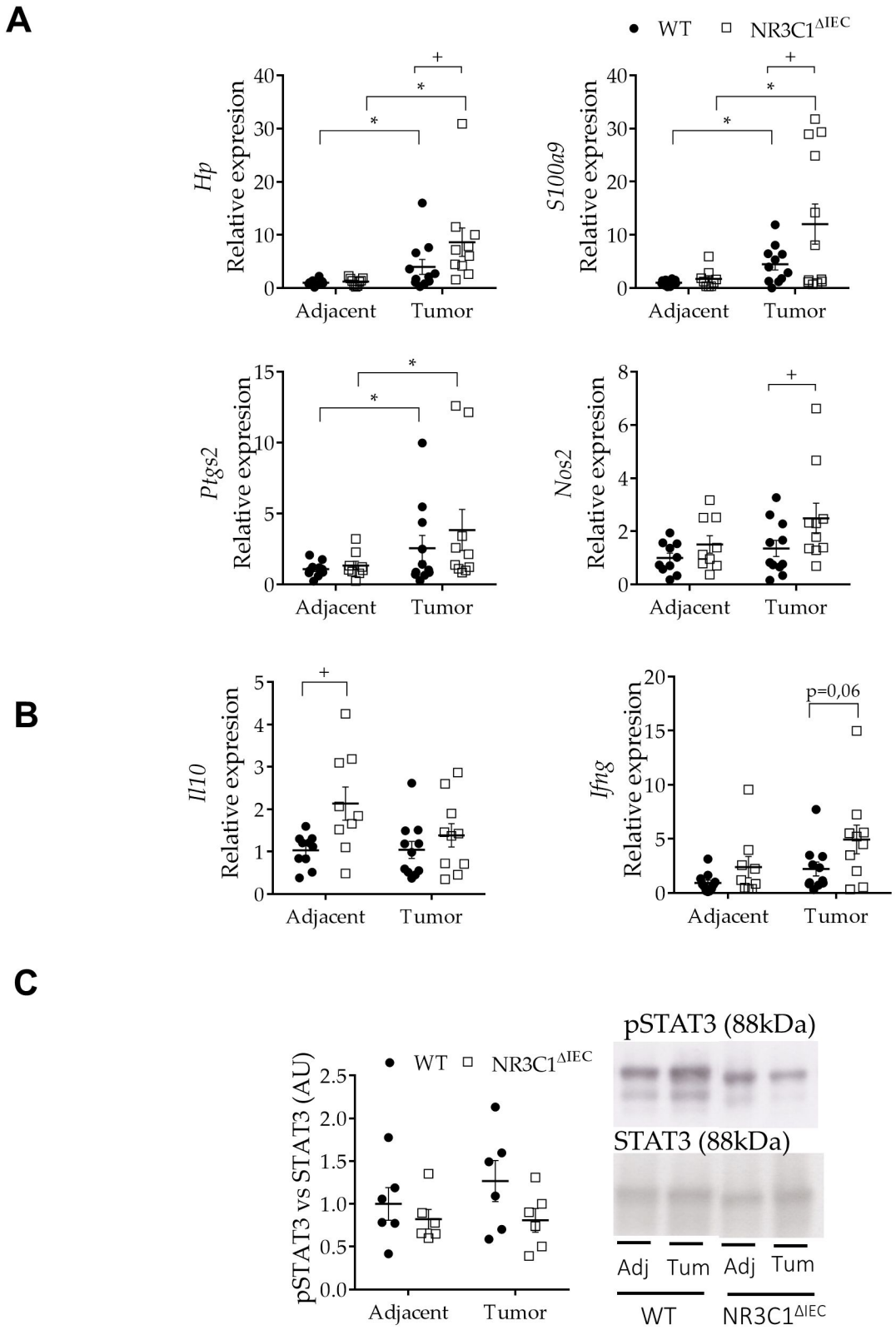
A
WT
NR3C1ΔIEC
Hp
S100a9
Ptgs2
Nos2
Relative expresion
Adjacent
Tumor
B
Il10
Ifng
p=0,06
C
pSTAT3 vs STAT3 (AU)
pSTAT3 (88kDa)
STAT3 (88kDa)
Adj
Tum
WT
NR3C1ΔIEC

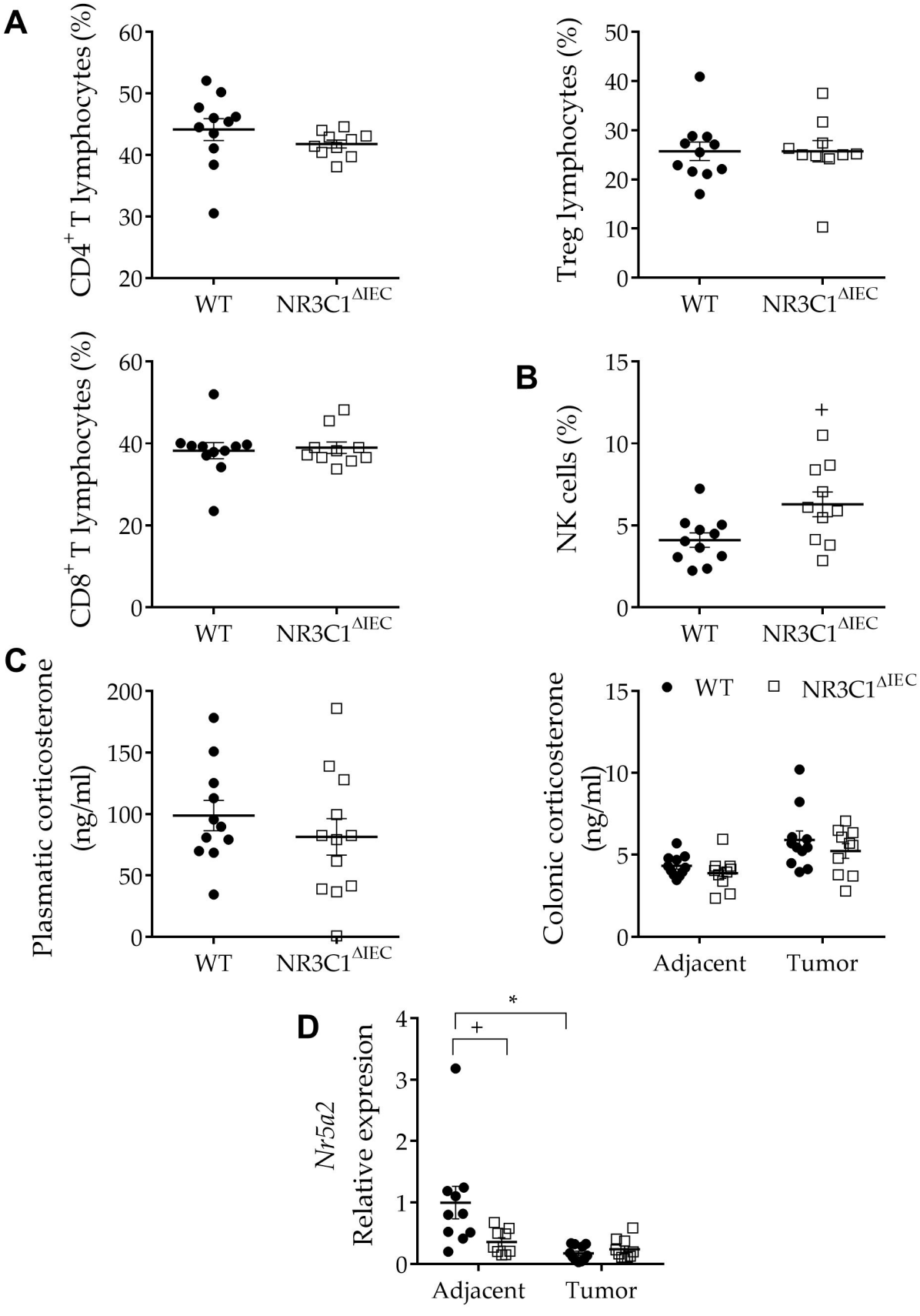
A
CD4+ T lymphocytes (%)
60
50
40
30
20
WT
NR3C1ΔIEC
Treg lymphocytes (%)
50
40
30
20
10
0
WT
NR3C1ΔIEC
CD8+ T lymphocytes (%)
60
40
20
0
WT
NR3C1ΔIEC
B
NK cells (%)
15
10
5
0
WT
NR3C1ΔIEC
C
Plasmatic corticosterone (ng/ml)
200
150
100
50
0
WT
NR3C1ΔIEC
Colonic corticosterone (ng/ml)
WT
NR3C1ΔIEC
15
10
5
0
Adjacent
Tumor
D
Nr5a2 Relative expresion
*
+
4
3
2
1
0
Adjacent
Tumor

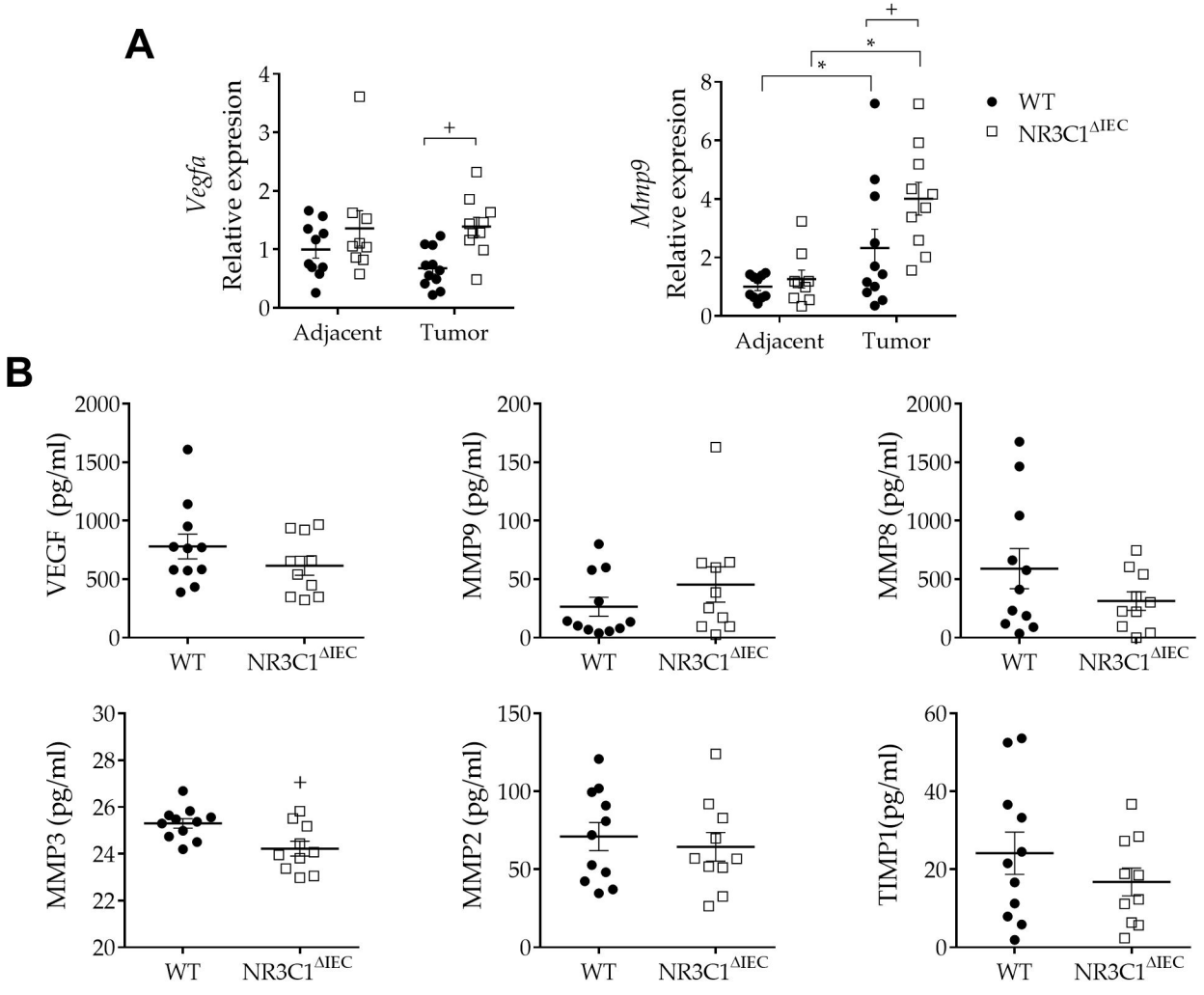
A
Vegfa
Relative expresion
4
3
2
1
0
+
Adjacent
Tumor
Mmp9
Relative expresion
8
6
4
2
0
+
*
*
Adjacent
Tumor
WT
NR3C1ΔIEC
B
VEGF (pg/ml)
2000
1500
1000
500
0
WT
NR3C1ΔIEC
MMP9 (pg/ml)
200
150
100
50
0
WT
NR3C1ΔIEC
MMP8 (pg/ml)
2000
1500
1000
500
0
WT
NR3C1ΔIEC
MMP3 (pg/ml)
30
28
26
24
22
20
+
WT
NR3C1ΔIEC
MMP2 (pg/ml)
150
100
50
0
WT
NR3C1ΔIEC
TIMP1(pg/ml)
60
40
20
0
WT
NR3C1ΔIEC